


A Numerical Adiabatic Model for the Quench Behavior Analysis of the Ag-Matrix Bi-2212 Round Wire

Chao Dai, Jaap J. Kosse, Hongwei Zhang, Li Liu , Jinggang Qin , Yu Wu, Huan Jin, Tongke Wang, Chao Zhou, and Sheng Liu

Abstract—To study the quench behavior of the Bi-2212 round wire as a promising superconductor for future fusion reactor coils and high-field magnets, a numerical adiabatic model has been developed at the Institute of Plasma Physics, Chinese Academy of Sciences. The model is in 1-D and the partial differential equation is solved with the implicit method. Quench energy is simulated by introducing heat in a section of the wire, and the temperature and voltage are calculated as the function of time and space. The minimum quench energy and normal zone propagation velocity were calculated at different conditions. The results from the model were compared with analytical solution and experiment data. The analysis and discussion are presented in this paper.

Index Terms—Bi-2212 round wires, implicit method, minimum quench energy (MQE), normal zone propagation velocity (NZPV), quench.

I. INTRODUCTION

FOR high-field magnet applications, new materials and techniques must be developed to replace the conventional Nb-based conductors. Bi₂Sr₂CaCu₂O_x (Bi-2212) is a promising candidate since it has high critical magnetic field and it is commercially available in round wire. Therefore, Bi2212 is taken into consideration to develop new conductors for future accelerator and fusion reactor applications. At the Institute of Plasma Physics Chinese Academy of Sciences (ASIPP), two small sizes Bi-2212 cable-in-conduit conductors (CICC) have been fabricated and tested [12], and a subscale insert coil will be designed to verify the high-field performance and homogeneity of the wire. One of the significant issues in the design is the stability

Manuscript received September 7, 2017; revised May 21, 2018; accepted May 23, 2018. Date of publication June 7, 2018; date of current version June 29, 2018. This work was supported by the National Magnetic Confinement Fusion Science Program under Grant 2014GB105001. This paper was recommended by Associate Editor L. Chiesa. (Corresponding author: Li Liu.)

C. Dai, J. Qin, Y. Wu, and H. Jin are with the Institute of Plasma Physics, Chinese Academy of Sciences, Hefei 230031, China.

J. J. Kosse and C. Zhou are with the Energy, Materials and Systems Faculty of Science and Technology, University of Twente 7500AE Enschede, The Netherlands.

H. Zhang and T. Wang are with the Tianjin Normal University, Tianjin 300387, China.

L. Liu is with the School of Information Science and Engineering, Dalian Polytechnic University, Dalian 116034, China (e-mail: liu.li@dpu.edu.cn).

S. Liu is with the China International Nuclear Fusion Energy Program Execution Center, Beijing 100862, China.

Color versions of one or more of the figures in this paper are available online at <http://ieeexplore.ieee.org>.

Digital Object Identifier 10.1109/TASC.2018.2841919

of the wire, which determines the quench protection strategy of a magnet. As an HTS conductor, the T_c of Bi2212 is much higher than low temperature superconductor (LTS) conductors, which leads to its normal zone propagation velocity (NZPV) being lower than LTS conductors and makes the quench detection more difficult. Due to these, it is necessary to investigate the quench behavior of Bi-2212 wires.

A numerical model for the quench behavior analysis of Bi2212 has been developed at Lawrence Berkeley National Laboratory [1]. In this study, a criterion was used to govern the current distribution, this method is simple and easy to process but is somewhat different from the actual situation. To solve the partial differential equation (PDE), an explicit method was used which is unstable if the time step is not small enough. In this paper, an improved model was developed. The major modification is the current-sharing model; the power law was used to govern the current sharing instead of the linear model. An implicit method was used to solve the PDE to avoid the instability. The minimum quench energy (MQE) and NZPV in various temperatures and magnetic fields were calculated using this model. This model can be used as a predictive model in future stability studies of the Bi-2212 CICC and magnets.

II. MODEL DESCRIPTION

The quench behavior numerical model is based on the thermal diffusion equation, which is a parabolic PDE

$$\gamma C \frac{\partial T}{\partial t} = \nabla \cdot (\kappa \nabla T) + P \quad (1)$$

where $T(x, t)$ is the spatially and temporally dependent temperature, and P is the volumetric heat flux, which includes heat generation such as Joule heating, heat exchange such as convective heat transfer, radiation heat transfer.

For superconducting wire, thermal diffusion is mainly along the axial direction, so 1-D form of this equation could describe the quench behavior of superconducting wire, which is given by

$$C^*(T) \frac{\partial T}{\partial t} = \frac{\partial}{\partial x} \left(\kappa^*(T, B) \frac{\partial T}{\partial x} \right) + I_n^2 \rho_{1d}(T, B) + P_i + P_c \quad (2)$$

where $C^*(T)$ is the specific heat capacity in 1-D in J/mK, the specific heat capacity data of Bi-2212 round wire is from [2], which is as a function of temperature. $\kappa^*(T, B)$ is the effective

thermal conductivity in Wm/K. Given the thermal conductivity of silver is several order of magnitude higher than the one of the Bi2212, it can be safely assumed that the heat conduction takes place only in the silver. Thermal conductivity of Ag is given by a polynomial from [3], [4], and the magnetic field is taken into account using

$$\kappa^*(T, B) = \kappa^*(T, 0) \cdot \frac{\rho(T, 0)}{\rho(T, B)} \quad (3)$$

where $\rho_{1d}(T, B)$ is the “1-D” electrical resistivity in Ω/m , which represents the electrical resistance per unit length, the temperature and magnetic field dependent electrical resistivity is taken from NIST [4], the magnetoresistance data of Ag can be reduced to a Kohler plot with the RRR of Ag.

The P_i is the initial power dissipation, which could cause an initial current sharing from filaments to matrix. If the P_i is high enough to cause a normal zone larger than minimum propagation zone (MPZ), the quench would propagate, and the P_i can be defined as

$$P_i(x, t) = \begin{cases} \delta(x) \frac{E_{\text{pulse}}}{t_{\text{pulse}}}, & 0 < t \leq t_{\text{pulse}} \\ 0, & t > t_{\text{pulse}} \end{cases} \quad (4)$$

the variable E_{pulse} is used to produce the quench energy and $\delta(x)$ is the Kronecker-delta function.

The cooling item P_c includes radiation and convective heat transfer, but the heat transfer coefficient h and emissivity ϵ are not known if there is no specific operating condition. Therefore, the cooling item is neglected in this model, that is to say the model is adiabatic.

In the previous work, the current in the normal area was calculated with a criterion T_{cs} , this model is ideal and assumes that it has a complete transient when the temperature exceeds the T_{cs} , which can be simply described by

$$\begin{aligned} I_n &= 0, & T &\leq T_{cs} \\ I_n &= I_{op} - I_{sc}, & T &> T_{cs} \end{aligned} \quad (5)$$

but in fact, for practical superconducting materials, the critical current inhomogeneity exists and it would cause nonlinear transient. The transient rate depends on a very important parameter, which is the n -index. In this study, the current-sharing model is replaced by a model which is closer to the actual situation. In this model, the current in nonsuperconducting element I_n , which can be obtained from the parallel path current-sharing model, which is represented in Fig. 1

$$I_n = I_{op} - I_{sc} \quad (6)$$

where I_{op} is the operating current, I_{sc} is the superconducting current, I_n is the current in the normal area, according to Ohm's law

$$I_n(i) = \frac{V_n(i)}{R_n(i)} = \frac{E_n(i) dx_i}{\rho_{1d}(i) dx_i} = \frac{E_n(i)}{\rho_{1d}(i)} \quad (7)$$

and

$$E_n = E_{sc} = E_c \left(\frac{J_{sc}}{J_c} \right)^n \quad (8)$$

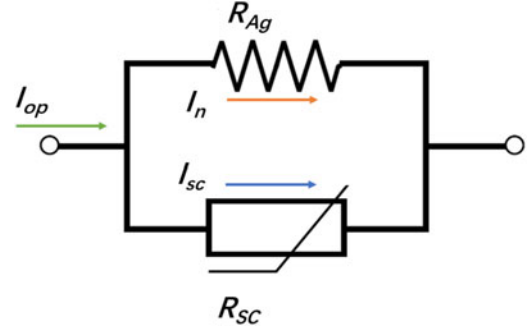


Fig. 1. Schematic representation of a superconductor with a normal conducting element in parallel with a superconducting element.

Then, (6) can be described numerically using the implicit expression

$$I_{op} - \frac{E_c}{\rho_{1d}} \left(\frac{J_{sc}}{J_c} \right)^n - I_{sc} = 0 \quad (9)$$

where E_c is the criterion (in this study it is $1e-4$ V/m), n is the n -index of the superconducting wire. Then, the I_{sc} can be achieved using a numerical search algorithm such as the Newton–Raphson method. In the equation, $I_c(T, B)$ is the temperature and magnetic field dependent critical current, which can be described with a model that is used to study current instabilities in Bi-based conductors [5], [6] and was introduced in [7] is used to fit the critical surface of the Bi-2212 conductor. The model is given by

$$\begin{aligned} I_c(T, B) &= I_0 \left(1 - \frac{T}{T_c} \right)^\gamma \left[\left(1 - \chi \right) \frac{B_0}{B_0 + B} \right. \\ &\quad \left. + \chi \exp \left(- \frac{\beta B}{(B_{c0} \exp(-\alpha T/T_c))} \right) \right] \end{aligned} \quad (10)$$

In the equation, following quantities are used: $T_c = 87.1$ K, $B_{c0} = 465.5$ T, $\alpha = 10.33$, $\beta = 6.76$, $\gamma = 1.73$, $\chi = 0.33$, and $B_0 = 1.0$ T, the parameters χ and I_0 are obtain by fitting the experimental data, and the remaining parameters are taken from [7]. After I_{sc} is determined, I_n can be calculated using (9), in Fig. 2 I_{sc} and I_n calculated with different models are plotted against T for a given I_{op} . From Fig. 2, it can be seen that compared with the linear schematic current-sharing model, this model gives a smoother transition taking place at T_{cs} and T_c , which is more approximate to the actual situation.

III. SOLUTION METHOD AND BOUNDARY CONDITION

A numerical method was used to solve the parabolic PDE, the numerical method includes explicit method and implicit method. For the explicit method, a scheme is called “forward time, centered space” is used. Explicit method is easy for calculation but it is proved unstable when the time step size is not small enough [8], that means a huge amount of data will be produced if the step size can satisfy stability requirement. Therefore, the implicit method which is proved unconditionally stable was used

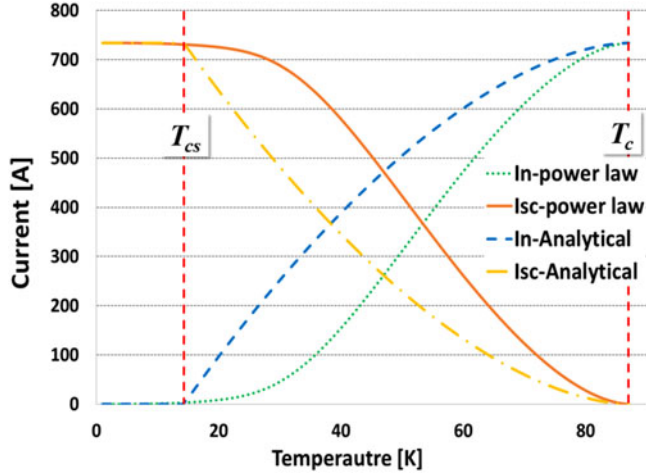


Fig. 2. I_{sc} and I_n with different current-sharing model are plotted against T for a given I_{op} [I_n and I_{sc} -analytical are calculated with (5) and I_n and I_{sc} -power law are calculated with (6)–(9)].

to solve [8]. Equation (11) is discretized as

$$C^*(T_i^n) \frac{T_i^{n+1} - T_i^n}{\Delta t} = \frac{1}{\Delta x} \left(\kappa^*(B, T_{i+1/2}^n) \frac{T_{i+1}^{n+1} - T_i^{n+1}}{\Delta x} - \kappa^*(B, T_{i-1/2}^n) \frac{T_i^{n+1} - T_{i-1}^{n+1}}{\Delta x} \right) + I_n^2(T_i^n) \rho^*(B, T_i^n) + P_{ini}. \quad (11)$$

In the equation, $T_{i+1/2}^n = \frac{1}{2}(T_{i+1}^n + T_i^n)$, and $T_{i-1/2}^n = \frac{1}{2}(T_i^n + T_{i-1}^n)$, and the code for the numerical method was written with Fortran.

For each node, I_n was calculated by the Newton–Raphson method, and P_{ini} is the initial power introduced into the node.

To solve (2), the initial and boundary conditions must be given. The initial condition of this model is set to be 4.2, 5, 7, and 9 K over the entire zone. For the boundary condition, as mentioned in the model description, the model is assumed to be adiabatic, the temperature at the ends of the wire is fixed to be same with the initial temperature, $\partial T/\partial x$ is forced to vanish at the boundaries.

IV. RESULT AND DISCUSSION

At present, the latest Bi-2212 round wire developed by the Northwest Institute for Nonferrous Metal Research has a critical performance $J_0 > 5500 \text{ A/mm}^2$. In the paper, $J_0 = 5000 \text{ A/mm}^2$ was used in the calculations. The models with the operating current I_{op} of $60\%I_c$ and $80\%I_c$ were calculated in various operating temperature and magnetic field. Figs. 3 and 4 show the temperature distribution of the recovered situation and the quenched situation, respectively.

A. Minimum Quench Energy

In order to simulate the MQE, an initial heat perturbation was introduced into a region of length $L_h = n_{node} * dx_i$ (dx_i is

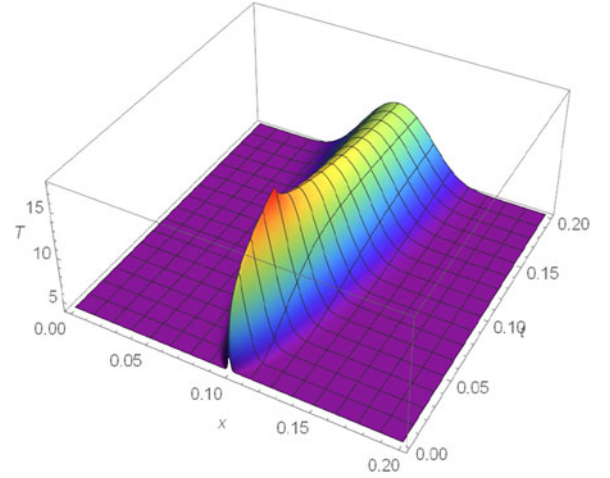


Fig. 3. Perturbation energy is lower the MQE, and the normal zone disappears again.

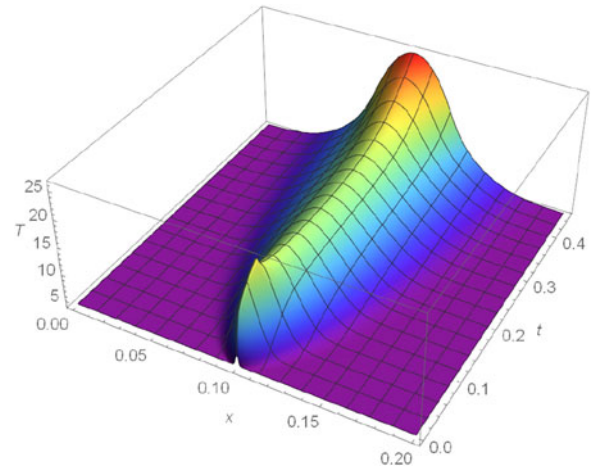


Fig. 4. Perturbation energy exceeds the MQE, and the quench propagation occurs.

the length between two adjacent nodes) during the heating time $t_h = \Delta t * n_{step}$ (in this paper, t_h is chosen to be 50 ms). Then, the perturbation heating energy can be calculated by $E_{pulse} = P_i * n_{node} * t_h$.

To find the MQE, a search algorithm can be used that runs the model multiple times. It requires an upper estimate and a lower estimate for the quench energy. First, the upper and lower estimates are tested to ensure that a quench occurs in the upper estimate and does not occur for the lower estimate. If the estimation proves to be incorrect, the upper and lower boundaries are adjusted automatically. After the upper and lower estimates have been confirmed, the energy exactly in between the upper and lower estimates is tried. If a quench occurs, the upper estimate is shifted toward the tested energy. If no quench occurs, the lower estimate is shifted. This process is repeated until the difference between the upper and lower estimates is less than a preset tolerance (for the calculation in this report, a tolerance of 0.1% is used). The minimal quench energy is then

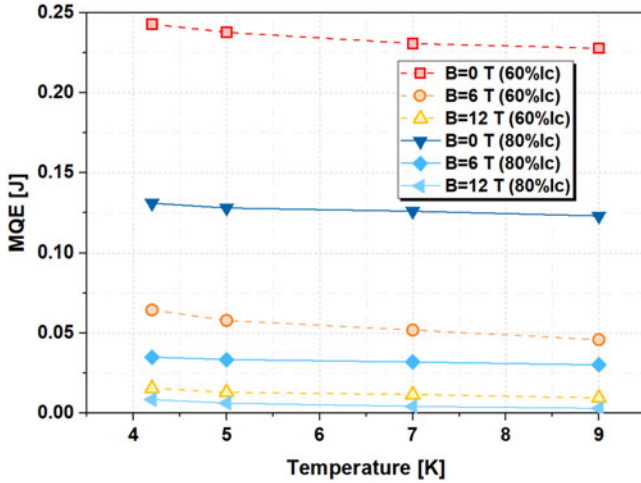


Fig. 5. MQEs calculated with numerical method are plotted against temperature at different magnetic fields and operating currents.

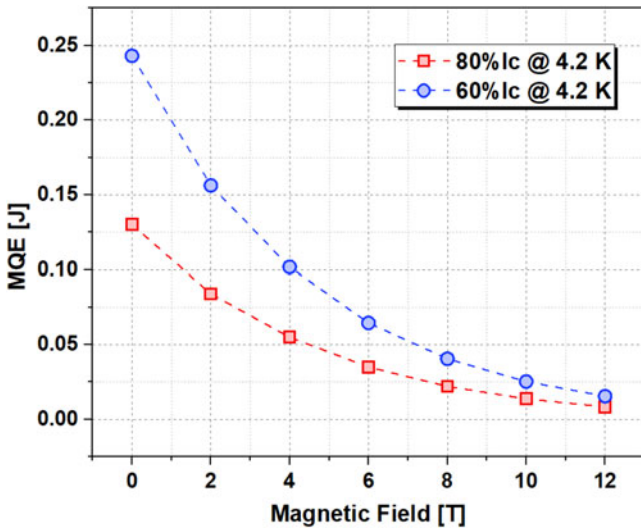


Fig. 6. MQEs calculated with numerical method are plotted against the magnetic field at 4.2 K.

equal to the upper estimate. The MQE of the wire in different temperatures and magnetic field are shown in Figs. 5 and 6.

From the figures, it can be seen that the MQE of the Bi-2212 round wire decreases with the increasing operating temperature and magnetic field. The results obtained by the numerical model are also compared with data measured by Ye *et al.* [9] and the MPZ model [10], [11]

$$\text{MQE} = \sqrt{\frac{2A^2 (T_{cs}(I) - T_{op})}{\rho_n I^2}} \int_{T_{op}}^{T_{cs}} C(T) dT. \quad (12)$$

The comparison is shown in Fig. 7, the numerical results (blue dots and red squares indicated as 80% I_c at 4.2 K and 60% I_c at 4.2 K) is an order of magnitude lower than the experimental results from [9], but is a considerable improvement compared to the MPZ model (yellow triangles). The deviation between numerical results and the experimental results can be foreseen because there are some differences between the model and experimental

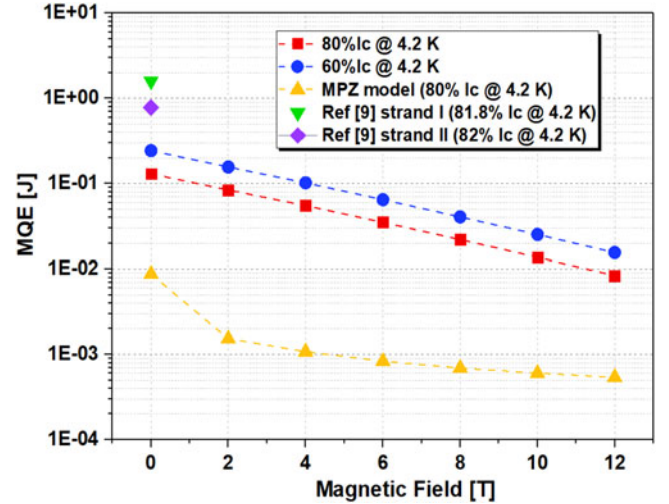


Fig. 7. Comparison of the MQE obtained by different methods.

condition. First, the MQE obtained by the experiments was by integrating the energy pulse, in the experiment, heaters made from silicon-insulated Nichrome wires are wound around the samples to induce quenches, and the heater was covered by Sty-cast 2850 epoxy [9], the entire sample was in the liquid helium bath. Thus, in the experiment, part of the energy generated by the heater was absorbed by liquid helium and epoxy, and the thermal resistance exists between the heater and the sample wire, which could cause heat dissipation, but different from the experimental condition, in the model, perturbation energy is fully absorbed by the nodes. Second, the boundary condition of the model is adiabatic, but in the experimental condition, heat transfer exists, both perturbation energy and Joule heat could dissipate into the liquid helium. These two factors caused the differences between the numerical and experimental results. The values calculated with classical MPZ model are much lower than numerical results because this model is relatively simple and qualitative, the parameters in the equation do not change with temperature.

B. Normal Zone Propagation Velocity

For calculating the NZPV, the voltage of the model should be calculated and a criterion should be determined ($1e-4$ V/m). The voltage of an area on the wire could be calculated by

$$U = \sum_{i=n}^m I_n(i) * \rho^*(i) * dx_i \quad (13)$$

where $I_n(i)$, $\rho^*(i)$, and dx_i are the normal zone current, the effective resistivity, and the length of node i . The calculated voltages of different areas on the wire are shown in Fig. 8.

The length of the normal zone l_n is then calculated at each time step using the two intersections between a horizontal line at the criterion and the calculated voltage. The normal zone velocity then becomes

$$V_{nzp} = \frac{dl_n}{dt}. \quad (14)$$

The calculated V_{nzp} at 4.2 K at various magnetic fields are also compared with the experimental data [9] and analytical

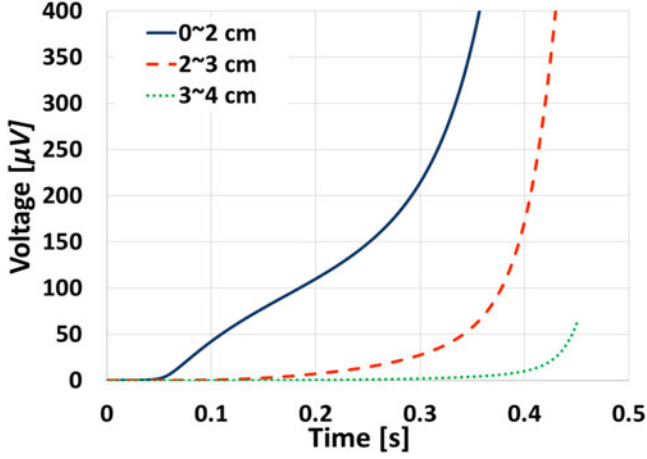


Fig. 8. Calculated voltages of different areas on the wire for 80% I_c and 12 T.

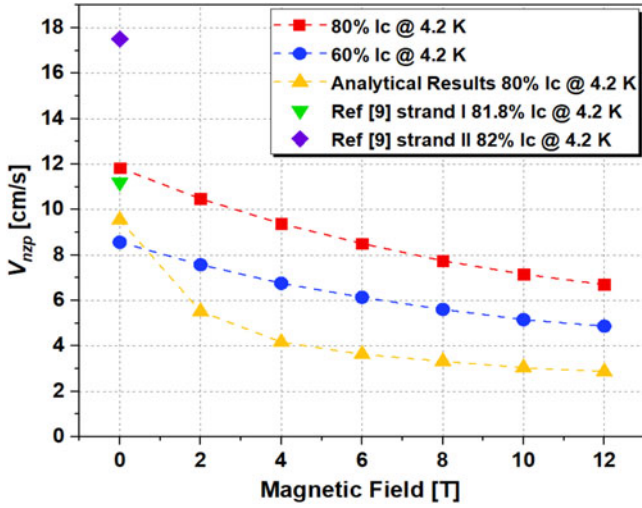


Fig. 9. Comparison of the NZPV obtained by different methods.

solution [11]

$$\text{NZPV} = J \sqrt{\frac{\rho_n \kappa_n}{C_n C_s (T_{cs} - T_{op})}} \quad (15)$$

the results are shown in Fig. 9.

The V_{nzp} decrease with the increasing magnetic field is due to the thermal conductivity of Ag decreasing as the magnetic field rises. Numerical result shows that the V_{nzp} of the 80% I_c at 0 T, 4.2 K is similar with the measured result. The difference between the two results could also be caused by the different boundary condition.

On the other hand, experiments are also necessary to validate the model. Now, an experimental device has been developed at ASIPP, this device is designed to study the MQE and V_{nzp} of superconducting samples at various magnetic fields and temperatures with quasi-adiabatic condition.

The device is designed as an insert that can be inserted into the background field magnet (with 65 mm bore) (see Fig. 10). The sample holder is filled with liquid helium which cools the current leads to 4.2 K. The sample holder is enclosed in a stainless steel

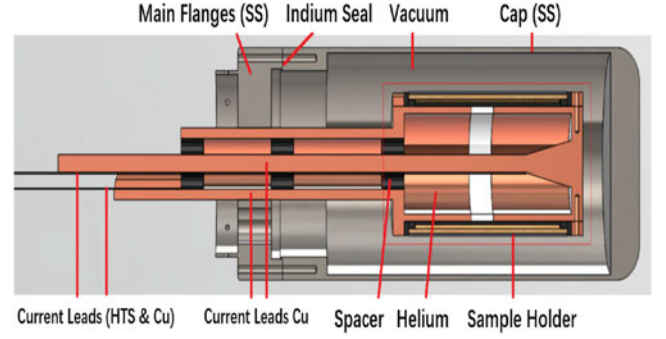


Fig. 10. Insert design schematic.

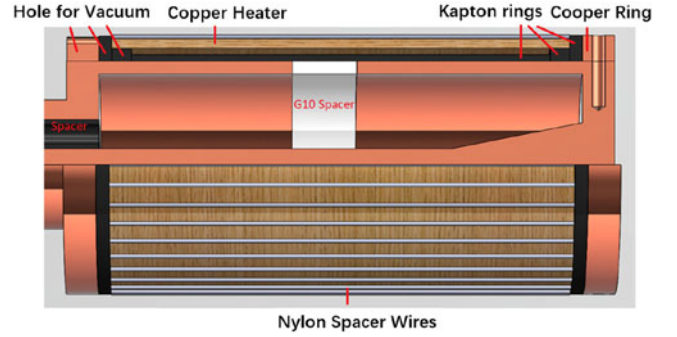


Fig. 11. Close-up schematic of the sample holder.

(316 L) cap which allows a vacuum to be applied around the sample (tube trough main flange for pumping is not shown). Because of this convective and conductive heat transfer of the sample with the helium is not present. Indium wire is used to make a leak free connection between the cap and the main flange (SS 316 L) [13].

A close-up of the sample holder is shown in Fig. 11. Nylon spacer wires reduce the thermal conductivity between the sample and the heater. This is needed to prevent any heat generated in a normal zone from transferring outside of the sample in the timescale of the quench propagation, so the quasi-adiabatic environment is made. The sample wire or tape can be wound outside the nylon spacer that ensures sample length is enough for propagation velocity measurement.

The device has been assembled and now is in the testing. We will study the quench behavior of Bi-2212 round wire at different conditions with this device and validate the numerical model.

V. CONCLUSION

A 1-D numerical model for simulating the quench behavior of Bi-2212 round wire was introduced in this paper. The implicit method was used to solve the PDE, and the power law model was used to describe the current sharing. MQE and NZPV at different conditions were calculated with this model. Calculated MQE is about one order of magnitude lower than the experimental result because the different boundary condition between the model and experiments and the different route to obtain the MQE. NZPV shows good agreement with the experiment result.

On the other hand, this model still has room for improvement. One is the difference between Ag and Ag/Mg alloy was neglected due to lack of the data of Ag/Mg alloy. The heater model will be upgraded by adding the thermal resistance between the heater and the wire and the heat transfer with liquid helium. A measurement device for studying the quench behavior at various temperature and magnetic field is in developing at ASIPP, the experiment results would provide the parameters of the cooling items to optimize the boundary condition of the numerical model.

REFERENCES

- [1] D. Arbelaez *et al.*, "Numerical investigation of the quench behavior of Bi2212 wire," *IEEE Trans. Appl. Supercond.*, vol. 21, no. 3, pp. 2787–2790, Jun. 2011.
- [2] C. S. Myers *et al.*, "Specific heats of composite Bi2212, Nb₃Sn, and MgB₂ wire conductors," *IEEE Trans. Appl. Supercond.*, vol. 23, no. 3, Jun. 2013, Art. no. 8800204.
- [3] Y. Iwasa *et al.*, "Magnetoresistivity of silver over temperature range 4.2–159 K," *Cryogenics*, vol. 33, no. 8, pp. 836–837, Aug. 1, 1993.
- [4] D. R. Smith and F. R. Fickett, "Low-temperature properties of silver," *J. Res. Nat. Inst. Stand. Technol.*, vol. 100, pp. 119–171, 1995.
- [5] V. R. Romanovskii and K. Watanabe, "Multi-stable static states of Bi-based superconducting composites and current instabilities at various operating temperatures," *Phys. C*, vol. 420, pp. 99–110, 2005.
- [6] V. R. Romanovskii, "Current instability mechanisms in high-temperature superconductors cooled by liquid coolant," *Supercond. Sci. Technol.*, vol. 23, no. 2, 2010, Art. no. 025020.
- [7] L. Bottura, "Critical surface for BSCCO-2212 superconductor," Note-CRYO/02/027, 2002.
- [8] G. Evans, J. Blackledge, and P. Yardley, *Numerical Methods for Partial Differential Equations*. London, U.K.: Springer, 2012.
- [9] L. Ye *et al.*, "On the causes of degradation in Bi2212 round wires and coils by quenching at 4.2 K," *IEEE Trans. Appl. Supercond.*, vol. 23, no. 5, Oct. 2013, Art. no. 6400811.
- [10] M. N. Wilson, *Superconducting Magnets*. Oxford, U.K.: Clarendon Press, 1983.
- [11] Y. Iwasa, *Case Studies in Superconducting Magnets: Design and Operational Issues*. New York, NY, USA: Springer Science & Business Media, 2009.
- [12] J. G. Qin *et al.*, "Manufacture and test of Bi-2212 cable-in-conduit conductor," *IEEE Trans. Appl. Supercond.*, vol. 27, no. 4, Jun. 2017, Art. no. 4801205.
- [13] J. J. Kosse, "Normal zone propagation set-up," Internal Report, 2013.

Authors' biographies not available at the time of publication.